

Solution of multi-component, two-phase Riemann problems with constant pressure boundaries

Thormod E. Johansen · Lesley A. James

Received: 5 March 2013 / Accepted: 14 December 2014 / Published online: 1 May 2015
© Springer Science+Business Media Dordrecht 2015

Abstract Riemann problems for two associated hyperbolic systems of conservation laws are considered. The Riemann problem for constant flow velocity finds existing solutions in the literature. Here, it is proved that the associated Riemann problem with the alternative assumption of constant pressure boundaries can be calculated from the constant velocity solution. This introduces the total velocity as an unknown function of time, which is explicitly determined in an algorithmic fashion.

Keywords Constant pressure boundaries · Hyperbolic systems · Riemann problems

1 Introduction

The Riemann problem was introduced by Riemann in [1] for systems of hyperbolic conservation laws describing gas dynamics [2, Chap. 18]. In Lax's comprehensive discussion of such systems [3], it was proved that for strictly hyperbolic systems (i.e., the eigenvalues of the system Jacobian are distinct), there is a unique solution of the Riemann problem provided the boundary data given by two constant states v^L and v^R are sufficiently close (in a precise sense). It has been demonstrated that Riemann problems for two-phase flow with multiple components typically are non-strictly hyperbolic. Nevertheless, some of these problems even with global data have been solved, e.g., [4,5].

The basis for this paper is a general model for flow of two immiscible fluid phases in a one-dimensional porous medium. Assuming the flow is also incompressible and dispersion free, the Riemann problem for this model is

$$(v + a(v))_t + f(v)_x = 0, \quad v(0, t) = v^L, \quad v(x, 0) = v^R, \quad (1)$$

where $x \in [0, L]$, $t \geq 0$, $v = v(x, t) \in \mathbb{R}^n$, and $a(v)$, $f(v) \in \mathbb{R}^n$ are given twice differentiable functions, and v^L , v^R are given constant states. We assume this system is hyperbolic, i.e., the eigenvalues of the Jacobian df are real. When the total volumetric flow rate (i.e., flow velocity) is also assumed to be constant, Riemann problems of the form (1) in some cases have known solutions, as will be reviewed in Sect. 2. In these cases, v represents overall component concentrations, f is a given component fractional flux function, and a is a given model for the stagnant component concentration, e.g., caused by components being adsorbed on the solid parts of the porous rock.

T. E. Johansen (✉) · L. A. James
Memorial University of Newfoundland, St. John's, Canada
e-mail: thormodj@mun.ca

The known solutions to the Riemann problem (1) only apply to the situations where the total volumetric flux is constant, in which cases the solutions of (1) are self similar, $v(x, t) = v(\xi)$; $\xi = x/t$. If instead the pressures at the medium boundaries $x = 0, x = L$ are kept constant, the volumetric flux will not be constant, and solutions will therefore not be self similar.

In this paper, we consider the following problem associated with (1):

$$(u + a(u))_t + U(t)f(u)_x = 0, \quad u(0, t) = u^L, \quad u(x, 0) = u^R, \quad p(0, t) = p^L, \quad p(L, t) = p^R, \tag{2}$$

The total volumetric flux $U(t) \geq 0$ is related to the pressure $p(x, t)$ through Darcy’s Law for the simultaneous flow of the two phases:

$$U(t) = -\Lambda(u)p_x, \tag{3}$$

where $\Lambda(u)$ is the total mobility of the fluid system. This total mobility is assumed to be known as a function of u . It is assumed to be a smooth function, as is supported by a vast amount of physical experiments. The function $U(t)$ in (2) is continuous, and p is piecewise differentiable in both x and t . Since we assume incompressible flow, there cannot be any fluid accumulation anywhere in the medium at any time. Therefore, U is a function of t only. Adding the pressure boundary data in (2) to the data in (1) could render the system overdetermined. However, in (2) $U(t)$ has become an unknown function as opposed to in (1) where $U \equiv 1$, and it is shown below that $U(t)$ in (2) is uniquely determined.

The main result of the paper is the following.

Theorem 1 *If the Riemann problem (1) has a solution v , the associated problem (2) also has a solution $u, p, U(t)$, where u is given by*

$$u(x, t) = v\left(\frac{x}{\Psi(t)}\right), \tag{4}$$

where

$$\Psi(t) = \int_0^t U(\tau) d\tau. \tag{5}$$

Furthermore, $U(t)$ is uniquely determined from $u(x, t)$ and the model boundary conditions, whereupon $p(x, t)$ is uniquely determined from (3).

The determination of $U(t)$ is given in Sect. 3. It is constructive in the sense that the function $U(t)$ is uniquely determined in an algorithmic fashion.

We first review the structure of solutions of Riemann problems (1). Such a solution consists of a sequence of $n + 1$ constant states $v^L = v_0, v_1, \dots, v_n = v^R$ separated by n elementary waves $w_i(\xi)$, each of which is a shock (or contact discontinuity) or a smooth rarefaction wave. If we denote the smallest and largest velocities for the i th wave by σ_i^- and σ_i^+ , respectively, the solution of (1) can be written

$$\begin{aligned} v^L = v_0; \quad & 0 \leq x \leq y_1 = \sigma_1^- t, \\ w_1(\xi); \quad & y_1 \leq x \leq x_1 = \sigma_1^+ t, \\ & \vdots \\ v_{i-1}; \quad & x_{i-1} \leq x \leq y_i = \sigma_i^- t, \\ w_i(\xi); \quad & y_i \leq x \leq x_i = \sigma_i^+ t, \\ & \vdots \\ v^R = v_n; \quad & \sigma_n^+ t = x_n \leq x \leq L. \end{aligned} \tag{6}$$

If the i th wave is a rarefaction wave,

$$\frac{dw_i(\xi)}{d\xi} = r_i(w_i(\xi)), \tag{7}$$

where $r_i \in \mathbb{R}^n$ is the right eigenvector of df corresponding to the eigenvalue λ_i . We also have $\sigma_i^- = \lambda_i(v_i)$; $\sigma_i^+ = \lambda_i(v_{i+1})$. If the i th wave is a shock, the classical Rankine–Hugoniot condition for material balance across a shock is

$$\sigma_i^+ = \sigma_i^- = \frac{[(f)_1]}{[(v)_1 + (a_1(v))_1]} = \dots = \frac{[(f)_n]}{[(v)_n + (a_n(v))_n]}, \tag{8}$$

where $(\)_j$ denotes vector components and $[\]$ is the jump in value across a shock.

We next describe the way the wave structures of (1) and (2) are related. Clearly, the right eigenvectors of df and $U(t)df$ are the same, and if λ is an eigenvalue of df , $U(t)\lambda$ is an eigenvalue of $U(t)df$. This defines the relationship between rarefaction waves for the two systems. Also, if σ is a shock velocity for (1) satisfying (8), $U(t)\sigma$ is a shock velocity for (2). Let (x, t) be given. For any wave value $w_i(x/t)$ for (1) with velocity σ ,

$$\frac{dx}{dt} = \sigma \quad \text{or} \quad x = \sigma \cdot t. \tag{9}$$

Since $U(t)$ is continuous, the location X of $w_i(x, t)$ in a solution of (2) is well defined and

$$\frac{dX}{dt} = U(t)\sigma \quad \text{or} \quad X = \Psi(t)\sigma. \tag{10}$$

Hence, since $U \equiv 1$ in (1) and v is self similar,

$$u(x, t) = v\left(\frac{1 \cdot t}{\Psi(t)}x, t\right) = v\left(\frac{x}{\Psi(t)}\right), \tag{11}$$

which proves (4). The remainder of the proof of the Theorem 1 is the construction of $U(t)$, which is given in Sect. 3. Once $U(t)$ is known, $p(x, t)$ follows from (3). We also formulate and prove two results on the smoothness of $U(t)$ in Sect. 3.

In Sect. 2, we discuss the previous literature related to Riemann problem of the form (1). In Sect. 4, we present a calculated example and compare the analytical solutions in this paper with numerical solutions obtained from a first-order finite-difference method.

2 Previous work

In addition to being useful in interpretation of core flood experiments with constant pressure boundaries, the results in this paper also offer applications in numerical simulation. For example, streamline simulation is frequently used by the oil industry to compute fluid flow in reservoirs between injectors and producers [6, 7]. In streamline simulations, the pressure distribution is first solved from an elliptic equation subject to simplifying assumptions. Subsequently, streamlines are generated using the pressures, and finally, the fluid flow between injectors and producers can be calculated analytically along streamlines, provided that the Riemann problem at hand has a known solution. The popularity of this approach is primarily because of considerable time savings compared to conventional simulations. Previous streamline simulations using solutions of Riemann problems along streamlines could only be performed for cases of constant flow rates. A more common way to operate wells is by keeping flowing well bore pressure constant. The solutions derived in this paper therefore widen the applicability of streamline simulations. Riemann

problem solutions can also be used as building blocks for the construction of numerical methods which can be used with general boundary conditions. Examples of this are the Random Choice Method, [8–10], and Godunov’s Method, [11].

Global solutions for many hyperbolic Riemann problems have yet to be found. A general theory for local existence and uniqueness of solutions of Riemann problems is described in [3] under the condition of strict hyperbolicity (distinct eigenvalues of the Jacobian).

However, flow phenomena in porous media are typically not strictly hyperbolic. The most well-known Riemann problem pertinent to the oil industry is the Buckley–Leverett theory for water injection in an oil reservoir [12, 13]. It is a single hyperbolic equation modeling the conservation of water. The conservation of oil is taken care of through the assumption of constant volumetric flux U both in space and time. Lake in [14, Chap. 5] gives a comprehensive description and easy to follow methodology for using and applying the Buckley–Leverett theory.

The first non-strictly multicomponent problem appearing in the literature with a complete global solution seems to be for single-phase (water) flow with dissolved components that adsorb on the rock in a nonlinear and coupled fashion, [4]. The adsorption causes a chromatographic separation of the individual components. A global solution of a non-strictly hyperbolic system modeling polymer flooding with nonlinear adsorption was presented in [15]. Here, the water phase contains dissolved polymer for the purpose of increasing the water viscosity to enhance sweep efficiency. Again, this was for constant volumetric flux in space and time. An example using this solution with constant pressure boundaries is presented in Sect. 4 of this paper.

A system with multiple adsorbing polymer components with decoupled adsorption was presented in [16]. This was generalized to a coupled adsorption model in [5]. A system describing four components, two-phase flow with components partitioning between the two phases was analyzed in [17, 18]. A comprehensive discussion and analysis of this is also presented in Orr [19, Chap. 5].

3 Construction of $U(t)$. Proof of Theorem 1

In this section, we will use the following notation for a solution of (2), see Eqs. (6) and (10):

$$\begin{aligned}
 v^L &= v_0; & 0 \leq X \leq Y_1 &= \Psi(t)\sigma_1^-, \\
 w_1(x, t); & & Y_1 \leq X \leq X_1 &= \Psi(t)\sigma_1^+, \\
 & & \vdots & \\
 v_{i-1}; & & X_{i-1} \leq X \leq Y_i &= \Psi(t)\sigma_i^-, \\
 w_i(x, t); & & Y_i \leq X \leq X_i &= \Psi(t)\sigma_i^+, \\
 & & \vdots & \\
 v^R &= v_n; & \Psi(t)\sigma_n^+ &= X_n \leq X \leq L.
 \end{aligned} \tag{12}$$

The construction of $U(t)$ consists of two main cases. If $t_{BT,i}$ is the time when the i th wave is breaking through at $x = L$, we consider

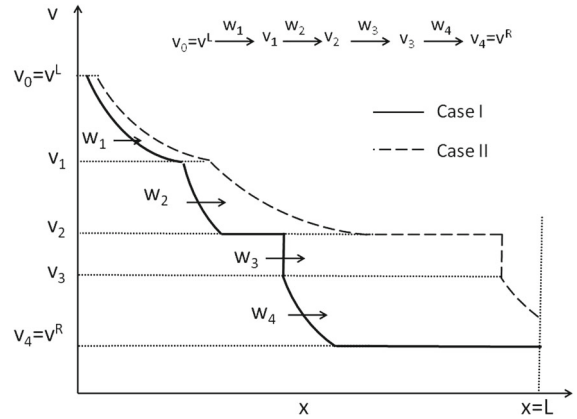
Case I: $t \leq t_{BT,n}$,

Case II: $t_{BT,n} \leq t \leq t_{BT,n-1}$.

The general result will then follow recursively from Case I and Case II, as will be explained at the end of this section.

Figure 1 shows an example with 4 waves w_1, w_2, w_3, w_4 separated by the sequence of constant states $v_o = v^L, v_1, v_2, v_3, v_4 = v^R$. Case I is at a time before the fastest wave w_4 breaks through at $x = L$ (i.e., $t \leq t_{BT,4}$), and Case II is at a time after the fastest wave w_4 has reached $x = L$ and before the following wave w_3 reaches $x = L$ (i.e., $t_{BT,4} \leq t \leq t_{BT,3}$).

Fig. 1 Example of waves and constant states



3.1 Case I. $t \leq t_{BT,n}$

Assume $u, U(t), p(x, t)$ is a solution of (2) and w_i is a rarefaction wave in u which we parameterize by $s \in [s_{i-1}, s_i]$; $w_i(s_{i-1}) = Y_i; w_i(s_i) = X_i$.

By (3),

$$p(Y_i, t) - p(X_i, t) = U(t) \int_{Y_i}^{X_i} \frac{dx}{\Lambda(w_i)}. \tag{13}$$

If λ_i is the eigenvalue of df corresponding to w_i , since f by assumption is twice differentiable, the eigenvalues of df are smooth and (10) gives

$$\frac{dX}{ds} = \Psi(t) \frac{d\lambda_i}{ds}. \tag{14}$$

Hence,

$$p(Y_i, t) - p(X_i, t) = U(t) \Psi(t) \int_{s_{i-1}}^{s_i} \frac{1}{\Lambda(w_i)} \frac{d\lambda_i}{ds} ds. \tag{15}$$

If w_i is a shock, then

$$p(Y_i, t) - p(X_i, t) = 0, \tag{16}$$

since p is continuous.

We define

$$\mathcal{J}_i = \begin{cases} 0 & \text{if } w_i \text{ is shock,} \\ \int_{s_{i-1}}^{s_i} \frac{1}{\Lambda(w_i)} \frac{d\lambda_i}{ds} ds & \text{if } w_i \text{ is rarefaction.} \end{cases} \tag{17}$$

Then, the following applies to both rarefactions and shocks:

$$p(Y_i, t) - p(X_i, t) = U(t) \Psi(t) \mathcal{J}_i. \tag{18}$$

When integrating (3) between $X = 0$ and $X = L$, we get (since in case I, $X_n \leq L$):

$$p^L - p^R = U(t) \left[\sum_{i=1}^{n-1} \left(\frac{Y_{i+1} - X_i}{\Lambda(v_i)} + \Psi(t) \mathcal{J}_i \right) + \frac{L - X_n}{\Lambda(v^R)} \right]. \tag{19}$$

We next use (10) to relate the end points Y_i, X_i of any wave to the leading edge of the fastest wave, X_n . From (10),

$$[Y_i, X_i] = [\sigma_i^- \Psi(t), \sigma_i^+ \Psi(t)], \quad (20)$$

and

$$X_n = \sigma_n^+ \Psi(t). \quad (21)$$

Hence,

$$\frac{dY_i}{dX_n} = \frac{\sigma_i^-}{\sigma_n^+} = \beta_i \quad \text{and} \quad \frac{dX_i}{dX_n} = \frac{\sigma_i^+}{\sigma_n^+} = \alpha_i, \quad (22)$$

where α_i, β_i are constants. Hence, since $X_i = Y_i$ at $t = 0$,

$$Y_i = \beta_i X_n; \quad X_i = \alpha_i X_n. \quad (23)$$

Substituting (23) in (19) and rearranging and also using $X_n = \Psi(t)\sigma_n^+$, we arrive at

$$\Delta p = U(t) \left[\left(\sum_{i=1}^{n-1} \left(\frac{\beta_{i+1} - \alpha_i}{\Lambda(v_i)} + \frac{\mathcal{J}_i}{\sigma_n^+} \right) - \frac{1}{\Lambda(v^R)} \right) X_n + \frac{L}{\Lambda(v^R)} \right]. \quad (24)$$

Solving (24) for $U(t)$ and substituting in (10),

$$\frac{dX_n}{dt} = U(t)\sigma_n^+. \quad (25)$$

Hence,

$$\frac{dX_n}{dt} = \frac{\Delta p \sigma_n^+}{AX_n + B}, \quad (26)$$

where $\Delta p, A, B$ are constants given by

$$\Delta p = p^L - p^R, \quad (27)$$

$$A = \sum_{i=1}^{n-1} \left(\frac{\beta_{i+1} - \alpha_i}{\Lambda(v_i)} + \frac{\mathcal{J}_i}{\sigma_n^+} \right) - \frac{1}{\Lambda(v^R)}, \quad (28)$$

$$B = \frac{L}{\Lambda(v^R)}. \quad (29)$$

Integrating the separable Eq. (26), we find an explicit expression for X_n as a function of time:

$$X_n = \frac{-B + \sqrt{B^2 + 4ACt}}{A}, \quad (30)$$

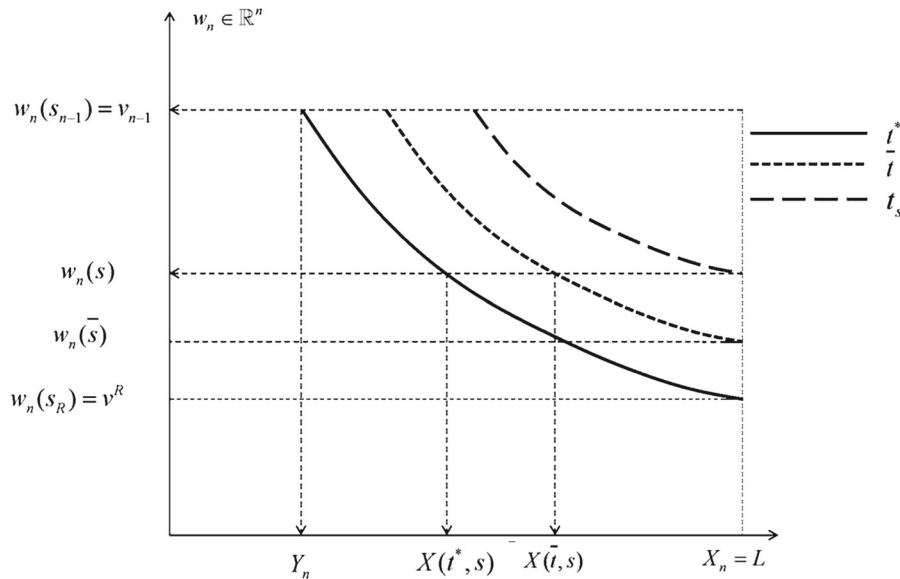


Fig. 2 The rarefaction wave at three different times after its leading edge has reached $x = L$

where

$$C = 2\Delta p\sigma_n^+ \tag{31}$$

The unknown velocity $U(t)$ is then determined explicitly from (24),

$$U(t) = \frac{\Delta p}{\sqrt{B^2 + 4ACt}} \tag{32}$$

The pressure distribution $p(x, t)$ can now be calculated from (3) using (32).

3.2 Case II. $t_{BT,n} \leq t \leq t_{BT,n-1}$

If w_n is a shock, $X_n = Y_n$. Therefore, in this case, v^R is no longer present in $[0, L]$ and the situation is identical to case I with $v^R := v_{n-1}$ and $n := n - 1$. It therefore suffices to consider w_n being a rarefaction wave. Let this smooth wave be parameterized by $s \in [s_{n-1}, s_R]$ with $w_n(s_{n-1}) = v_{n-1}$ and $w_n(s_R) = v^R$. Let s be arbitrary but fixed in this interval, and let t_s be the time when $w_n(s)$ reaches $X = L$. We will next determine $U(t_s)$ which will complete case II since s was arbitrary. Let t^* be the time when the leading edge of w_n reaches L , i.e., $X_n = L$. Let $X(s, t^*)$ be the location of $w_n(s)$ at $t = t^*$. Let $\bar{t} \in [t^*, t_s]$ be arbitrary. The movement of w_n is depicted in Fig. 2 as three profiles at times t^* , \bar{t} and t_s vs. X .

In order to capture the dynamics of the system, it is necessary to determine $U(\bar{t})$; $\bar{t} < t_s$ and then,

$$U(t_s) = \lim_{\bar{t} \rightarrow t_s} U(\bar{t}).$$

Let \bar{s} be the parameter for which $X_n(\bar{s}) = L$ at $t = \bar{t}$. Then, by (10), similar to (19) with w_n being a rarefaction wave,

$$\Delta p = U(\bar{t}) \left[\sum_{i=1}^{n-1} \frac{Y_{i+1} - X_i}{\Lambda(v_i)} + \Psi(\bar{t}) \sum_{i=1}^{n-1} \mathcal{J}_i + \Psi(\bar{t}) \int_{s_{n-1}}^{\bar{s}} \frac{1}{\Lambda(\omega_n)} \frac{d\lambda_n}{ds} ds \right] \tag{33}$$

Using (10),

$$\Psi(\bar{t}) = \frac{X(\bar{t}, s)}{\lambda_n(s)} \quad (34)$$

and

$$U(\bar{t}) = \frac{1}{\lambda_n(s)} \frac{dX(\bar{t}, s)}{dt}. \quad (35)$$

Similar to (22), we define

$$\frac{dY_i}{dX(\bar{t}, s)} = \beta_i; \quad \frac{dX_i}{dX(\bar{t}, s)} = \alpha_i \quad (36)$$

and find

$$Y_i = X(\bar{t}, s)\beta_i; \quad X_i = X(\bar{t}, s)\alpha_i. \quad (37)$$

In (33), we substitute (34) for $\Psi(\bar{t})$, X_i and rearrange, to arrive at

$$X(\bar{t}, s) \frac{dX(\bar{t}, s)}{dt} = \frac{\Delta p \lambda_n^2(s)}{A_1 \lambda_n(s) + B_1 + \int_{s_{n-1}}^{\bar{s}} \frac{1}{\Lambda(\omega_n)} \frac{d\lambda_n}{ds} ds}, \quad (38)$$

where

$$A_1 = \sum_{i=1}^{n-1} \frac{\beta_{i+1} - \beta_i}{\Lambda(v_i)}; \quad B_1 = \sum_{i=1}^{n-1} \mathcal{J}_i. \quad (39)$$

Integrating (33) between t^* and \bar{t} and letting $\bar{t} \rightarrow t_s$, we find

$$X(t^*, s)^2 - L^2 = \frac{2\Delta p \lambda_n(s)^2 (t_s - t^*)}{A_1 \lambda_n(s) + B_1 + \int_{s_{n-1}}^s \frac{1}{\Lambda(\omega_n)} \frac{d\lambda_n}{ds} ds}. \quad (40)$$

We then go back to (30), from which we can calculate t^* (with $X_n = L$). Furthermore,

$$X(t^*, s) = \Psi(t^*)\lambda_n(s). \quad (41)$$

Therefore, (40) provides an explicit expression for t_s . Re-introducing $U(t_s)$ in (40), we find

$$U(t_s) = \frac{X(t^*, s)^2 - L^2}{2L\lambda_n(s)(t_s - t^*)}. \quad (42)$$

To summarize, t^* is calculated from (30), then t_s is calculated from (40), and finally $U(t_s)$ from (42). Since s was arbitrary, this completes Case II.

The two above cases complete the proof of Theorem 1, since once the fastest wave is no longer present in $[0, L]$, we can repeat the construction of $U(t)$ with $v^R = v_{n-1}$; $n := n - 1$.

In this section, we finally discuss and prove a Proposition on the smoothness of the total velocity $U(t)$. This is done by considering the critical times when the leading and trailing points (X_i and Y_i) of different waves pass the outlet end $X = L$ of the medium.

It is not immediately clear that (42) is consistent with the fundamental equations in (10) as $t_s \rightarrow t^*$. However, we have

$$\begin{aligned} \lim_{t_s \rightarrow t^*} \frac{dX(t^*, s)}{dt} &= \lim_{t_s \rightarrow t^*} \frac{X(t^*, s) - L}{t^* - t_s} = \lim_{t_s \rightarrow t^*} \frac{X^2(t^*, s) - L^2}{(X(t^*, s) + L)(t^* - t_s)} \\ &= \lim_{t_s \rightarrow t^*} \frac{X^2(t^*, s) - L^2}{2L(t^* - t_s)} = U(t^*)\lambda(s_R). \end{aligned} \tag{43}$$

The result then follows from the fact that U is continuous and w_n is a rarefaction wave with continuous eigenvalue λ .

Proposition 1 *The solution $U(t)$ in Theorem 1 is differentiable when a shock wave w_n passes the outlet end $X = L$ if and only if*

$$\frac{\sigma_n^+}{\Lambda(v_n)} = \frac{\sigma_{n-1}^+}{\Lambda(v_{n-1})}. \tag{44}$$

Proof The terms in (24) were expressed using X_n . Let t^* be the time where the shock reaches $X = L$. For $t > t^*$, X_n is no longer meaningful, and we instead express the terms in (24) using X_{n-1} since X_{n-1} is present in the system after t^* . Let

$$g_B(t) = \sum_{i=1}^n \left(\frac{\bar{\beta}_{i+1} - \bar{\beta}_i}{\Lambda(v_i)} + \frac{1}{\sigma_{n-1}^*} \mathcal{J}_i \right) x_{n-1} + \frac{L - \bar{\alpha}_n X_{n-1}}{\Lambda(v_n)}, \tag{45}$$

where $\bar{\beta}_i, \bar{\alpha}_i$ are the quantities in (22) expressed in terms of X_{n-1} . Then, with reference to (22), $U(t)$ before X_n reaches $x = L$ is $\Delta p/g_B(t)$. Similarly, after x_n has reached $x = L$, we define

$$g_A(t) = \sum_{i=1}^n \left(\frac{\bar{\beta}_{i+1} - \bar{\beta}_i}{\Lambda(v_i)} + \frac{1}{\sigma_{n-1}^*} \mathcal{J}_i \right) x_{n-1} + \frac{L - X_{n-1}}{\Lambda(v_{n-1})}, \tag{46}$$

with $\Delta p/g_A(t)$ being $U(t)$ after X_n has reached $x = L$. We note that $g_A(t^*) = g_B(t^*)$ and find

$$\left(\frac{dU}{dt} \right)^+ (t^*) = -\frac{\Delta p g'_A(t^*)}{g_A^2(t^*)} = \frac{\Delta p}{g_A^2(t^*)} \left[k_1 - \frac{\bar{\alpha}_n}{\Lambda(v_{n-1})} \right] X'_{n-1}(t^*) \tag{47}$$

and

$$\left(\frac{dU}{dt} \right)^- (t^*) = -\frac{\Delta p}{g_B^2(t^*)} \left[k_1 - \frac{1}{\Lambda(v_{n-1})} \right] X'_{n-1}(t^*), \tag{48}$$

where k_1 is constant.

Hence, $U'(t^*)$ exists if and only if

$$\frac{\bar{\alpha}_n}{\Lambda(v_n)} = \frac{1}{\Lambda(v_{n-1})}, \tag{49}$$

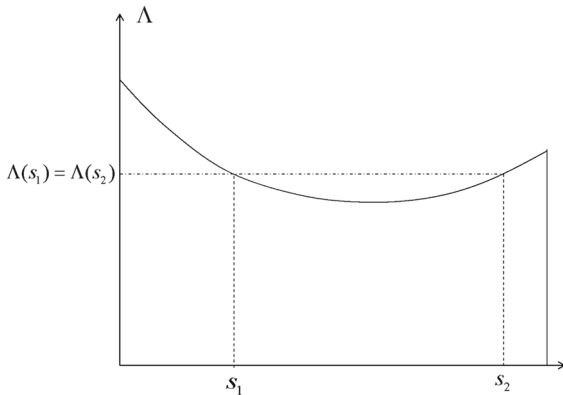


Fig. 3 Λ versus saturation

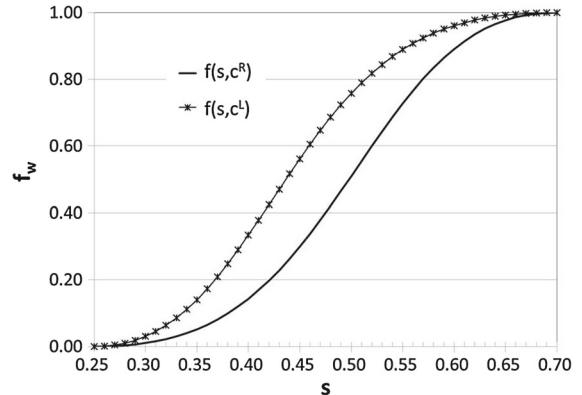


Fig. 4 Fractional flow functions

or

$$\frac{\sigma_n^+}{\Lambda(v_n)} = \frac{\sigma_{n-1}^+}{\Lambda(v_{n-1})}. \tag{50}$$

This proves Proposition 1. □

Corollary 1 *The function $U(t)$ is differentiable during the time interval when a rarefaction wave (or a constant state) passes the outlet at $X = L$.*

Proof By continuity, for a rarefaction wave, the relationship (44) is satisfied as an infinitesimal shock. □

The relationship (37) is in general not valid for a shock, although it may happen coincidentally. An example on this is as follows:

Assume that a shock w_n is followed by a rarefaction w_{n-1} such that $\sigma_{n-1}^+ = \sigma_n^+$. Then, (50) means that $\Lambda(v_n) = \Lambda(v_{n-1})$, i. e. the total mobility is the same on both sides of the shock. Typically, Λ for a single conservation law has the shape depicted in Fig. 3, where s_1, s_2 are parameter values on each side of a shock, and (50) is satisfied.

4 Calculated examples

In the oil industry, The Buckley–Leverett solution (1941) is synonymous with fractional flow theory where an immiscible fluid displaces another in one-dimensional flow in a porous medium. Physically, fractional flow theory describes the linear displacement of one phase by another immiscible phase where there is a front described by a shock or sudden change in concentration. In its simplest form, it describes one component displacing another immiscible component in one dimension in the absence of diffusive and compressible flow, i.e., water displacing oil [12, 13]. Mathematically, the Buckley–Leverett equation is a first-order hyperbolic partial differential conservation equation in time and space.

We give an example on how the theory in this paper can be applied to a polymer flooding case where the viscosity of the water phase is linearly dependent on the concentration of polymer added.

In addition to demonstrating the computational algorithm, the purpose of this example is to demonstrate the significant difference between the solutions based on the constant flow rate assumption, and the constant pressure boundary assumption of this paper. Furthermore, a grid sensitivity study is presented using a first-order finite-difference approximation, comparing the analytical and numerical solutions.

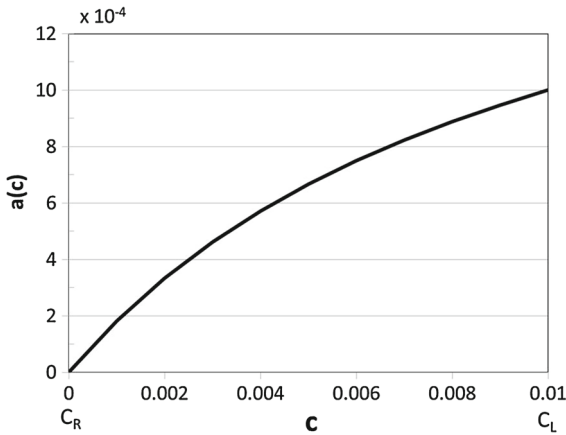


Fig. 5 Adsorption function

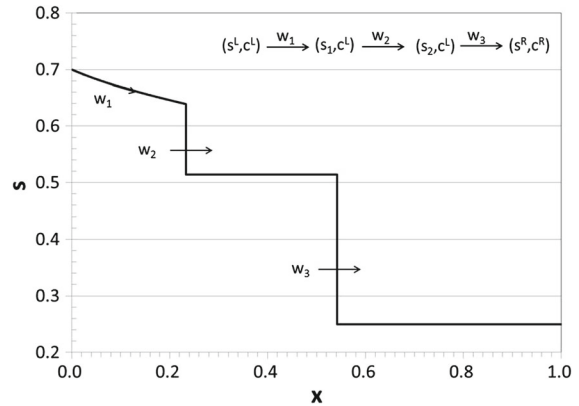


Fig. 6 Saturation profiles at a fixed time

The example is based on the results of [15], where the constant flow rate assumption is used to analyze the Riemann problem for polymer flooding with nonlinear adsorption. This provides the Riemann problem solution (1) needed for the construction of $U(t)$ in Theorem (1).

The hyperbolic system of conservation laws for this polymer flooding process is

$$s_t + f(s, c)_x = 0, \quad [sc + a(c)]_t + [f(s, c)]_x = 0, \tag{51}$$

where $t \geq 0$; $x \in \mathbb{R}$; the state vector $(s, c) \in I \times I$ represents water saturation and polymer concentration. Furthermore $f : I \rightarrow \mathbb{R}$ and $a : I \rightarrow \mathbb{R}$ are twice differentiable functions modeling the fractional flux of the water phase and polymer adsorption on the rock surface, respectively. We use the following explicit expressions:

$$f(s, c) = \frac{s^2}{s^2 + (0.5 + 100c)(1 - s)^2}, \tag{52}$$

$$a(c) = \frac{0.2c}{1 + 10c}. \tag{53}$$

The functions f and a are graphed in Figs. 4 and 5 for $c \in [0.00, 0.01]$.

We consider the Riemann problem for (51) with $s^R = 0.25$; $s^L = s_o = 0.70$; $c^L = 0.01$; $c^R = 0.00$. The solution is detailed in [15] and shown in Fig. 6 at a fixed time.

The solution is composed of three waves. The slowest wave is a rarefaction (v_1) corresponding to the eigenvalue $\partial f / \partial s$. The middle wave (v_2) is a shock corresponding to the eigenvalue $f / (s + a'(c))$, and the fastest wave is a shock (v_3) corresponding to the eigenvalue $\partial f / \partial s$.

The waves are separated by two constant states, $s_1 = 0.639$ and $s_2 = 0.514$. The integrals in (17) are $\mathcal{J}_2 = \mathcal{J}_3 = 0$ since waves 2 and 3 are shocks, and the coefficients A, B, C in (28), (29), (31) are easily obtained by numerical integration and summarized in Table 1:

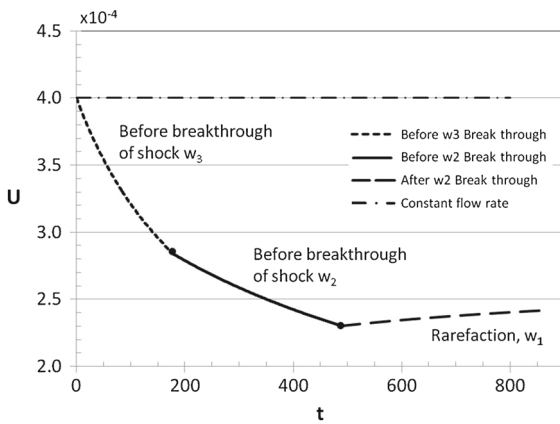
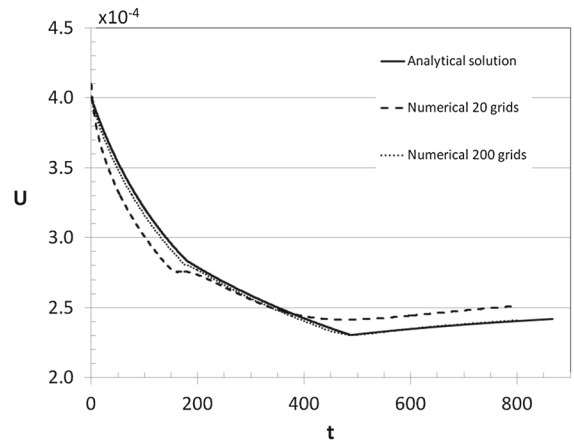
$$A = 1 - \frac{v_2}{v_3} \frac{1}{\lambda_T(s_2, c^R)} + \frac{1}{v_3} \mathcal{J}_1 - \frac{1}{\lambda_T(s^R, c^R)}, \quad B = \frac{L}{\lambda_T(s^R, c^R)}, \quad C = \frac{2\Delta p}{\phi} v_3. \tag{54}$$

The solution $U(t)$ of Theorem 1 for the above Riemann problem is shown in Fig. 7, together with the constant flow rate solution with $U(t) \equiv 0.89$. As can be seen, the constant pressure boundary solution $U(t)$ decreases from 0.89 initially to 0.50 at the minimum and then increases to 0.53. Clearly, it represents a big error to use the constant flow rate solution in an approximation for a constant pressure boundary case.

A numerical simulation of the polymer case was also carried out using a first-order upwind method with implicit treatment of pressure and explicit treatment of saturation. Figure 8 shows the variation in numerical versus analyti-

Table 1 Integration coefficients for the example (see text)

Integration coefficient	After first shock breakthrough	After second shock breakthrough
A	4.11×10^9	5.75×10^9
B	1.0×10^{10}	1.16×10^{10}
C	1.35×10^8	5.80×10^7

**Fig. 7** Solution in Theorem 1 for the example**Fig. 8** Numerical solution compared to analytical solution in Fig. 6

cally computed total volumetric flux results. The simulations were performed with 20 and 200 grid points As Fig. 8 indicates, a reasonable resolution of $U(t)$ is obtained using 200 grid points.

5 Conclusions

Existing solutions to global Riemann problems with constant volumetric flux have been extended to constant pressure boundaries with variable flux. The derivation mathematically describes the explicit behavior before the first wave breaks through, between waves and post breakthrough of the trailing rarefaction waves. The continuity and smoothness of the flux is also described. The application of the constant pressure boundary solution is illustrated with an example on polymer flooding.

References

1. Riemann B (1896) *Gesammelte Werke*. Dover Books, New York, p 149
2. Smoller J (1982) *Shock waves and reaction–diffusion equations*. Springer, New York
3. Lax PD (1957) Hyperbolic systems of conservation laws II. *Commun Pure Appl Math* 10:537–566
4. Rhee H-K, Aris A, Amundson NR (1970) On the theory of multicomponent chromatography. *J Philos Trans R Soc Lond Ser A* 267:419–455
5. Dahl O, Johansen T, Tveito A, Winther R (1992) Multicomponent chromatography in a two phase environment. *SIAM J Appl Math* 52(1):65–104
6. Bratvedt F, Gimse T, Tegnander C (1996) Streamline computations for porous media flow including gravity. *Trans Porous Media* 22:517–533
7. Thiele M, Batycky RP, Fenwick DH (2010) Streamline simulation for modern reservoir engineering workflows. *J Pet Technol* 62:64–70
8. Chorin AI (1976) Random choice solutions to hyperbolic systems. *J Comput Phys* 22:517–533

9. Concus P, Proskurowski (1979) Numerical solutions of a nonlinear hyperbolic equation by the random choice method. *J Comput Phys* 30:153–166
10. Glimm J (1965) Solutions in the large for nonlinear hyperbolic systems. *Commun Pure Appl Math* 18:697–715
11. Godunov SK (1959) A finite difference method for the numerical computation of discontinuous solutions of the equations of fluid dynamics. *Math USSR Sb* 47:271–290
12. Buckley SE, Leverett MC (1941) Mechanism of fluid displacement in sands. *Pet Trans AIME* 146:107
13. Welge HG (1952) A simplified method for computing oil recovery by gas or water drive. *Pet Trans AIME* 195:91
14. Lake LW (1989) *Enhanced oil recovery*. Prentice-Hall, Englewood Cliffs, NJ, USA
15. Johansen T, Winther R (1988) The solution of the Riemann problem for a hyperbolic system of conservation laws modelling polymer flooding. *SIAM J Math Anal* 19(3):451–566
16. Johansen T, Winther R (1989) The Riemann problem for multicomponent polymer flooding. *SIAM J Math Anal* 20:909–929
17. Johansen T, Wang Y, Orr FM Jr, Dindoruk B (2005) Four-component gas/oil displacement in one dimension: part I: global triangular structure. *Trans Porous Media* 61:59–76
18. Wang Y, Dindoruk B, Johansen, Orr FM Jr (2005) Four-component gas/oil displacement in one dimension. Part II: Analytical; solutions for constant equilibrium ratios. *Trans Porous Media* 61:177–192
19. Orr FM Jr (2007) *Theory of gas injection processes*. Tie-Line Publication, Copenhagen